IOP Publishing New J. Phys. 27 (2025) 045001 https://doi.org/10.1088/1367-2630/adc6b0

New Journal of Physics
The open access journal at the forefront of physics

Deutsche Physikalische Gesellschaft DPG
IOP Institute of Physics

Published in partnership with: Deutsche Physikalische Gesellschaft and the Institute of Physics

OPEN ACCESS

RECEIVED
20 December 2024

REVISED
14 March 2025

ACCEPTED FOR PUBLICATION
28 March 2025

PUBLISHED
9 April 2025

PAPER

Fast switching of the rf trapping field in an ion trap

Laura Blackburn*, Amber Shepherd and Matthias Keller

Department of Physics and Astronomy, University of Sussex, Brighton, BN1 9QH, United Kingdom
* Author to whom any correspondence should be addressed.

E-mail: laura.blackburn@sussex.ac.uk

Keywords: ion trap, switching, REMPI, loading

Abstract

Radiofrequency ion traps are essential for many experiments, ranging from quantum computing to physical chemistry and fundamental science. However, in some circumstances the trapping fields may cause undesired effects and need to be switched off briefly during operation without compromising the trap stability. By employing interference in the trap resonator circuit to enable switching faster than the resonator's natural decay, the electric field in the trap can be extinguished by >50 dB. We have demonstrated that it is possible to switch a linear Paul trap off for several microseconds without the loss of $^{40}Ca^{+}$ ions, even for large three-dimensional ion crystals, and have examined the effect of the switching parameters on the ion dynamics by monitoring the fluorescence rate. We have loaded N_2^{+} ions into a crystal of trapped calcium ions via photoionisation using this technique, demonstrating that it is also possible to capture ions despite the absence of a trapping field during the ionisation.

1. Introduction

Ion trapping allows unrivalled localisation and control of atomic and molecular ions, with diverse applications that include quantum computing [1, 2], metrology [3–5], precision spectroscopy for tests of fundamental physics [6, 7], and chemical reaction studies [8]. In recent years, the advent of new techniques and improved control [9, 10] have broadened the scope of such experiments to include polyatomic molecular ions [11–15] and exotic species such as highly charged ions [16, 17]. The desire for controlled experiments with increasingly complex ions brings challenges in producing these ions in well-defined internal states and trapping them alongside additional auxiliary ions for sympathetic cooling [18] and detection [9].

While the rf trap is essential to these experiments, the electric fields of the trap itself may compromise some processes. An example of this is producing molecular ions via state-selective photoionisation within the trapping region. In near-zero electric fields, such ionisation processes can have state preparation fidelities of >99% for ionisation into the desired state, e.g. [19]. However, in strong electric fields, field ionisation of Rydberg states below the ionisation threshold can reduce the state-selectivity [20–22]. The high spatial and temporal gradients of the electric field in a typical rf ion trap are sufficient to significantly limit the achievable fidelity of state-selective loading by this method, even when the laser pulses are synchronised to a zero crossing of the rf oscillation [23, 24].

One solution to this is to ionise molecules at or very close to zero field by extinguishing the rf field in the trap for a short time. This is a viable approach if three conditions are met: 1. any existing trapped ions are not lost or excessively heated; 2. any newly generated ions are captured; and 3. in the case of preventing field ionisation, the trapping field is extinguished for longer than the lifetimes of any high-lying Rydberg states susceptible to field ionisation [23]. For low frequency traps, digital operation can allow a period of low field [25], and methods for switching the electric fields in ion traps and guides are well-established in mass spectrometry applications [26–30]. We previously demonstrated another technique that is well-suited for switching the electric fields in high-frequency rf traps driven by high-Q-factor resonators. This technique uses interference with high-amplitude rf signals to switch the electric trapping field off and on again faster than the natural decay and recovery times of the high-Q resonator, which can be many tens of microseconds

for typical circuits. We showed that this technique enabled a short period of low field and that it was possible to retain ions in a Paul trap during this process [23].

In this work, we have built on this result by adapting the technique to minimise the field amplitude for longer times; examining the effect of switching on the dynamics of $^{40}Ca^{+}$ ions in a linear Paul trap; and investigating whether molecular nitrogen ions can be loaded into the trap during this process. We found that existing ions were retained for switching times of several microseconds and recooled within a few tens of milliseconds after switching, for both small and large crystals. We have also demonstrated that it is possible to capture nitrogen ions produced via resonance-enhanced multiphoton ionisation (REMPI) whilst the trap field is switched.

2. Fast extinction and recovery of the trapping field

2.1. Methods

We have used the technique implemented in [23] to switch the trap drive in a linear Paul trap consisting of four radial rf electrodes and two axial dc electrodes (figure 1(a)). Holes in the axial electrodes provide access for lasers along the axis of the trap.

The trap was driven at 22.09 MHz using a resonator circuit with a Q-factor of 260, corresponding to a natural switch-off time of several tens of microseconds. Under normal operation, the resonant circuit was driven by an rf signal via the primary coil of a transformer (figure 1(b)). The secondary coil of the transformer was connected to two diametric radial electrodes via 6.7 nF capacitors. The capacitors are part of a bias-tee to combine the trap drive with dc voltages for micromotion compensation via parallel 2 MΩ resistors. The remaining two radial electrodes were connected via 6.7 nF capacitors to ac ground and combined with dc compensation voltages via parallel 1 MΩ resistors. The resonator circuit was monitored by a pick-up coil, located close to the transformer, which was used to quantify and optimise the extinction of the field.

The trap was driven asymmetrically, by applying rf voltages to only one pair of radial electrodes while the other pair was held at rf ground. Due to the finite length of the electrodes, this resulted in confinement of the ions in all three dimensions using only the rf field. This simplified the switching process, as otherwise it would have been necessary to switch off the axial dc voltages when working with multiple ions. Voltages were applied to the axial electrodes only for the purpose of compensating stray fields. Micromotion was compensated in all three axes of the trap for all experiments by applying dc voltages to all six electrodes.

In this work, we have used the interference of additional drive signals with the intra-resonator field to achieve faster-than-natural decay and recovery of the trap field during switching. In this scheme, three function generator outputs provided the normal trap drive, FG 1, a higher amplitude out-of-phase drive for fast extinction, FG 3, and a higher amplitude in-phase drive for fast recovery of the field, FG 2 (figure 2(a)). Three rf switches, activated by a pulse generator that was synchronised to the phase of the rf drive, controlled which of these rf inputs (or ground) were transmitted to the resonator. A bandpass filter (Mini Circuits BBP-21.4) was used to remove ringing noise, which occurred at the pulse edges. The output from the switches passed via a 100 W amplifier (Mini Circuits ZHL-100W-GAN+) to the resonator circuit. The signal from the pick-up coil was used to monitor the rf amplitude during switching of the trap and to determine the extinction ratio. The voltage on the pick-up coil was converted to the electrode voltage using a calibration from the measured secular frequency of the ion, assuming an ideal trap geometry.

During switching, the normal trapping field was extinguished using the out-of-phase high-amplitude drive and then, once the field was minimised, recovered by a high-amplitude drive in-phase with the normal trap drive (figure 2(b)). To minimise the field for longer times, an additional pulse was added for which the rf electrodes were grounded (figure 2(c)).

2.2. Results and discussion

It was possible to extinguish the electric field in the trap by >50 dB when switching with both the simple and extended methods (figure 3). The duration for which the trap was considered off in the simple case was approximately half of the period of the rf signal. For the extended case, the off period can be arbitrarily long, although the dynamics of the ions will limit what is practical.

The quality of the extinction of the field is dependent on the phase and timings of the rf drives, which must be tuned to achieve the highest extinction. The speed with which it is possible to switch the trap off and on again depends on the natural decay time of the resonator, which is proportional to the Q factor and inversely proportional to the drive frequency of the resonant circuit. As the natural decay time increases relative to the desired extinction time, the rf powers required for extinction and recovery increase exponentially. The required powers also increase linearly with the normal drive power. In many cases, the

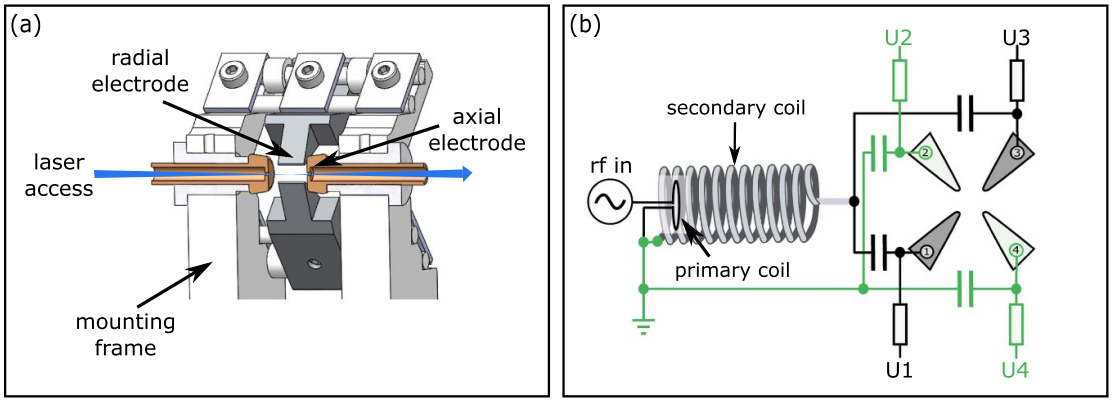

Figure 1. (a) Cross-section of the ion trap, showing the electrodes and laser access along the axis of the trap. Radiofrequency signals are applied to two of the four radial electrodes to confine the ions. We applied dc voltages to each of the six electrodes for micromotion compensation. (b) Resonator circuit used to generate the rf voltages on the radial electrodes. An rf signal was applied to the primary coil of a resonant transformer, the secondary coil of which was connected to radial electrodes 1 and 3. Electrodes 2 and 4 were held at rf ground. Bias tees, each consisting of a capacitor and resistor, were used to combine the rf drive with dc micromotion compensation voltages, U1-4, on each of the electrodes.

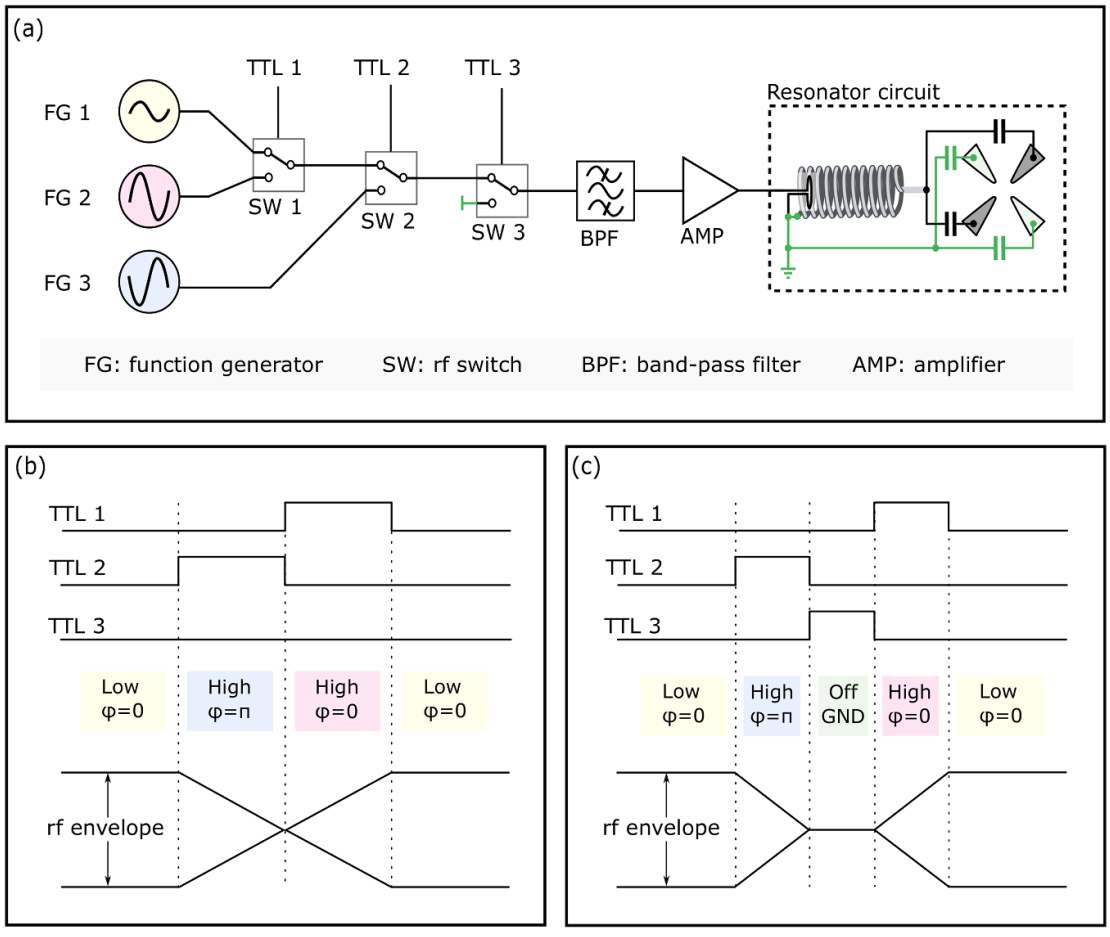

Figure 2. Method for fast extinction and recovery of the trapping field. (a) The trap is driven via three rf switches and a 100 W amplifier. The three rf switches are used to switch the rf signals between FG 1, FG 2, FG 3 and ground. These switches are controlled by TTL pulses from a delay generator, where the connections shown in part (a) correspond to when all TTLs are low. The FG signals have the same frequency, but different amplitude and phase. The full resonator circuit is shown in figure 1(b), and simplified here for clarity. (b) In the simplest implementation, two TTLs are used extinguish and recover the trapping field. (c) In the extended implementation, a third TTL is used to extend the time for which the electric field in the trap is minimised before recovery.

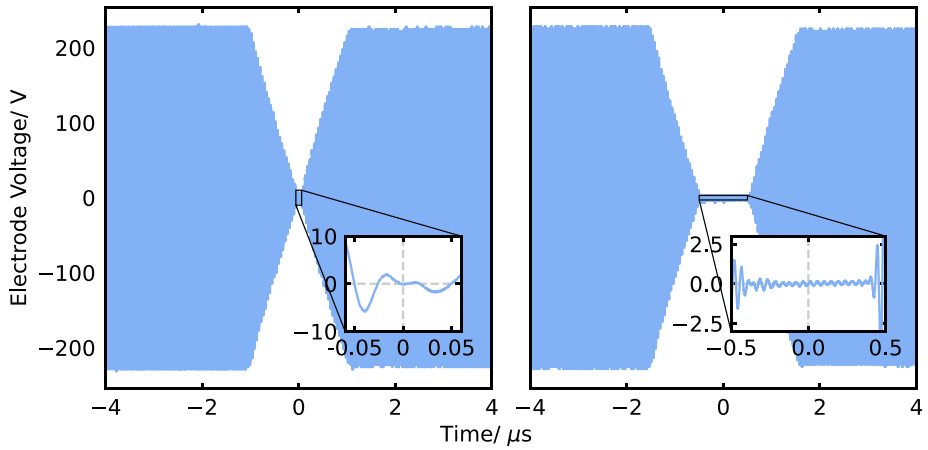

Figure 3. Extinction of the rf electric field in the ion trap during switching. (a) The electrode voltage during simple switching of the trap field (see figure 2(b)). (b) The electrode voltage during extended switching of the trap field (see figure 2(c)).

capacity of the amplifier will therefore limit the achievable switching times. It should be noted that significant reflections from the resonator can occur during switching, necessitating the use of a robust amplifier.

The shape of the falling and rising rf envelope is approximately linear when the extinction and recovery times are short relative to the decay time. To achieve the same gradient for the rising and falling slopes, the in-phase drive (FG 2) needs to be significantly larger than the amplitude of the destructive drive (FG 3). As an example, the data in figure 3 were taken with input powers to the resonator circuit of (2.8 ± 0.2) W for the normal drive, (26 ± 2) W for the out-of-phase drive and (50 ± 3) W for the high-amplitude in-phase drive.

3. Dynamics of existing ions

3.1. Methods

We investigated the dynamics of trapped ions during fast switching of the trap (as described in section 2) by observing the fluorescence rate of trapped $^{40}Ca^{+}$ ions.

The calcium ions were loaded from a resistively heated oven below the trap, using lasers at 423 nm and 375 nm for ionisation. The ions were cooled by addressing the $S_{1/2} \rightarrow P_{1/2}$ transition at 397 nm, using lasers at 850 nm and 854 nm to repump population out of the $D_{3/2}$ and $D_{5/2}$ states to close the cooling cycle (figure 4(a)). Photons emitted from the $P_{1/2}$ and $P_{3/2}$ states at 397 nm and 393 nm respectively were collected by a 0.27 NA lens, filtered and detected by a photomultiplier tube (PMT).

During the measurements, a time-to-digital converter (TDC) was used to record a histogram of photon counts, correlated to the switching of the trap. The 'start' signal for the TDC was provided by a pulse generator, PG 1 (figure 4(b)). The TTL signals for the trap switching were generated by a second pulse generator, PG 2, which was triggered via a synchronisation device to ensure synchronisation with the phase of the trapping field. The pulses from PG 2 were delayed by approximately 15 ms from the start of the TDC measurement to provide a fluorescence reference for the measurement before the trap was switched. Pulses generated by the PMT, resulting from the detection of single photons, were timestamped by the TDC to construct a histogram of photon counts correlated to the rising edge of the first TTL used in the switching process. The data in each histogram was accumulated over many cycles of switching.

Switching resulted in heating of the ions, with post-switching fluorescence rates initially reduced before recovering to the original rate [31, 32]. A general logistic function was fitted to the latter part of this recooling curve to extract a Doppler recooling time, which we define as the time taken to recover to 95% of the original fluorescence rate after the initial switching pulse edge. We have used this recooling time to quantify the impact of the switching technique on the ions without evaluating the entire recooling process.

In the following measurements, the recooling time was measured for different switching parameters and numbers of ions. The simple switching implementation (figure 2(b)) was used to investigate the effects of the extinction time and rf amplitude, and the extended implementation (figure 2(c)) was used to examine the effects of the off time and crystal size. The parameters used for the different measurements are shown in table 1. The secular frequencies, corresponding to different amplitudes of the rf trapping field, were determined using the crystal weighing technique described in [33]. For switching with a large 3D crystal, the trap was switched 100 times at a rate of 1 Hz. In all of the other measurements, the trap was switched 250

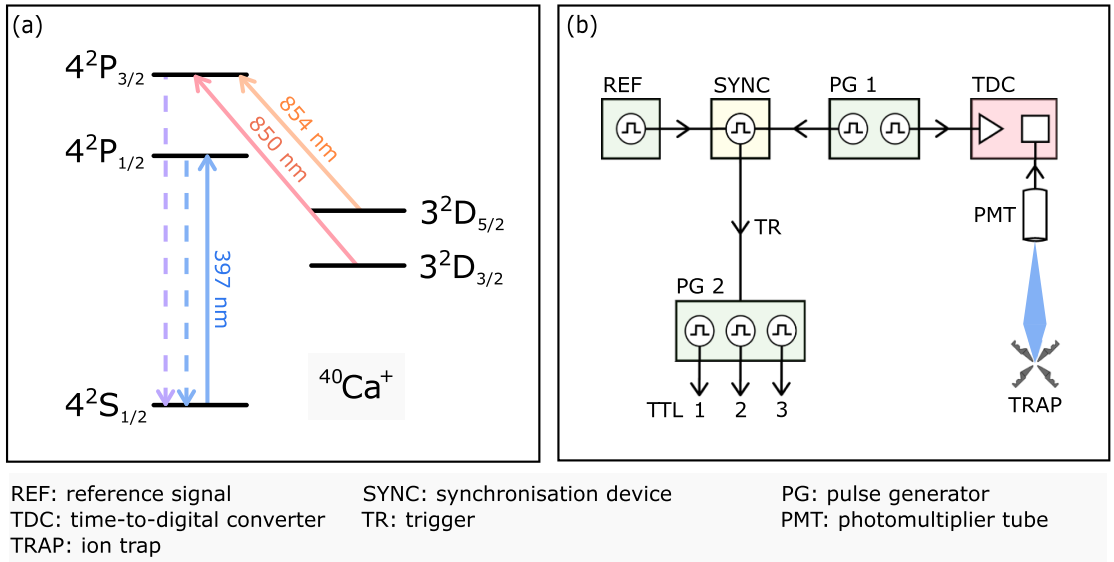

Figure 4. (a) Energy level diagram of $^{40}Ca^+$ showing the lasers used for Doppler cooling. (b) The set-up used to measure the heating of trapped ions during switching of the rf trap drive. A pulse generator, PG 1, triggers the start of the TDC measurement and a second pulse generator, PG 2, via a synchronisation device. This synchronised the trigger for PG 2 to a reference signal, REF, at a subharmonic of the trap drive. PG 2 provides the TTLs for the switching, as in figure 2(a). Photons fluoresced by the ion crystal were detected by the PMT and timestamped by the TDC to build a histogram of photon counts correlated to the switching process over many cycles of switching.

Table 1. Settings used for switching measurements in figures 5, 6.

Measurement	Extinction time (μs)	Off time (μs)	$\omega_r/2\pi$ (kHz)
Extinction time (figure 5(a))	—	0.0	360
Off time (figure 5(b))	1.0	—	360
ω_r (figure 5(c))	2.5	0.0	—
Number of ions (figure 6)	1.0	1.0	360

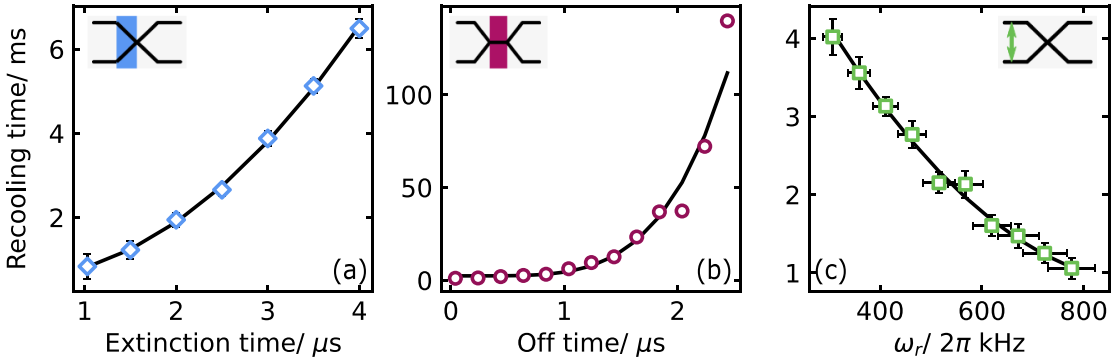

Figure 5. Effect of timing and rf amplitude on ion heating during switching, shown with polynomial fits to the data. (a) The time taken for the fluorescence of a single ion to recover after switching for different extinction times, where the recovery time was equal to the extinction time in each case. Inset, a schematic indicating the extinction time. (b) The time taken for the fluorescence of a single ion to recover after switching for different off times. Inset, a schematic indicating the off time. (c) The time taken for the fluorescence of a single ion to recover after switching for different secular frequencies of the ion, corresponding to different amplitudes of the rf trapping field. Inset, a schematic indicating the rf amplitude.

times at a rate of 1 Hz and the cooling laser detuning and power were kept constant. The ion crystal was laser cooled for the duration of the measurement in all cases.

3.2. Results and discussion

As the extinction and recovery time increased, the time taken for a single ion to recool after the trap was switched off and on again also increased (figure 5(a)). Notably, for an extinction time of 1 μs, corresponding to a total switching time of 2 μs, a single ion required less than 1 ms to recool to its original temperature.

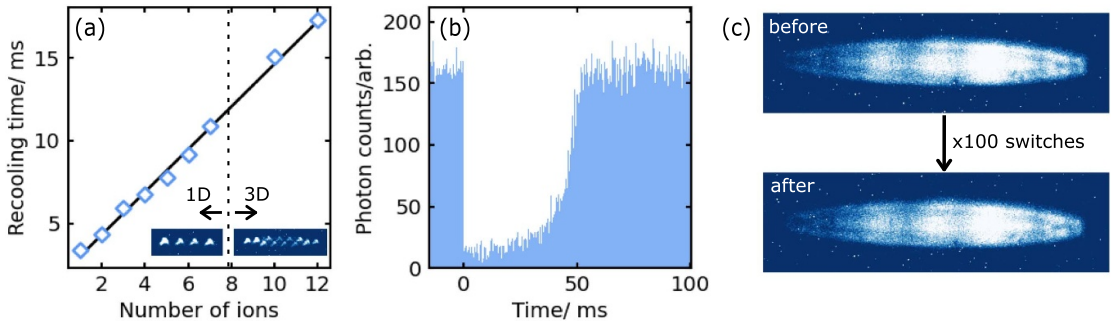

Figure 6. Effect of ion number on heating during switching. (a) The time taken for the fluorescence of an ion crystal to recover after switching for different numbers of ions. Inset, CCD images of 1D and 3D ion crystals recorded during the switching measurements, with an exposure time of 2 s. (b) Histogram of photon counts correlated to the leading edge of the switching process, for a large 3D ion crystal. (c) CCD images of the large 3D crystal, before and after the switching measurement in (b).

Using the extended switching method, the recooling time for a single ion increased as the off time increased (figure 5(b)). The recooling time remained below 10 ms for off times below about 1.2 μs, beyond which it increased more steeply reaching 130 ms recooling time for 2.2 μs off time. Hence, for shorter off times the trap can be switched off without significant heating. Even where the ion temperature was highest with 2.5 μs off time, the probability of losing the ion in a single switching event was very low, with the ion surviving 250 consecutive switching events at 1 Hz during the measurement. As the off time increased further, the probability of losing the ion during 250 cycles of switching was no longer negligible for off times greater than approximately 2.7 μs. For constant extinction and recovery times, the recooling time decreased with increasing rf amplitude for a single ion (figure 5(c)). Notably, approximately doubling the confinement during normal operation reduced the recooling time from (4.0 ± 0.2) ms to (1.1 ± 0.1) ms.

The trend lines in figure 5 show polynomial fits to the data. For the extinction time and rf amplitude these were dominated by the quadratic term, and for the off time the fit was dominated by the quartic term. While this system appears to be simple, the ion's motion moves from an adiabatic regime at high confinement into a strongly non-adiabatic regime close to the field extinction, which complicates the modelling of the dynamics. In addition, the dominant source of heating is likely to be due to electronic noise from the attached voltage supplies, weighted towards very low frequencies which are relevant for the ion close to where the amplitude of the trapping field is minimised. The source of the fast increase in ion temperature with increasing off-time is unclear. In particular, the fast increase in recooling time is not consistent with a simple coupling of the ion to a noise source.

The recooling time increased with the number of ions for both 1D and 3D crystals (figure 6(a)). Large 3D crystals of many tens of ions were found to have typical recooling times of tens of milliseconds (e.g. figures 6(b) and (c)). The effect of additional ions can be modelled using the analytical equations in [31], taking the initial energy to be the minimised potential energy of the Coulomb crystal. While this approximation breaks down for small energies, the simulated trend in recooling time is approximately linear where it holds, consistent with the trend observed experimentally (figure 6(a)).

Switching using the simple implementation results in less heating than the extended method, but the achievable off time is only about half the period of the rf field. On the other hand, it is possible to achieve off times up to e.g. 2.5 μs using the extended off-time implementation, but at the expense of $>100\times$ greater ion recooling time. The extent of the heating can be reduced by increasing the rf amplitude but, in practice, this strategy is likely to be limited by the capacity of the amplifier. For switching parameters where significant heating occurs, the detuning and power of the cooling laser can be tuned to minimise the recooling time. The scaling of recooling time with number of ions was approximately linear, making this technique feasible even for large crystals of many tens, and even 100s, of ions.

This method of switching is generally applicable to ion traps driven by resonant circuits, including multipolar traps. In this work, we have trapped the ions using only rf confinement to isolate its effect on the ions, but in many linear ion traps it may not be possible to trap without dc voltages on the axial electrodes. In these cases, the dc voltages must be switched off and on again while maintaining continuous compensation of stray fields to prevent excessive heating and loss of ions.

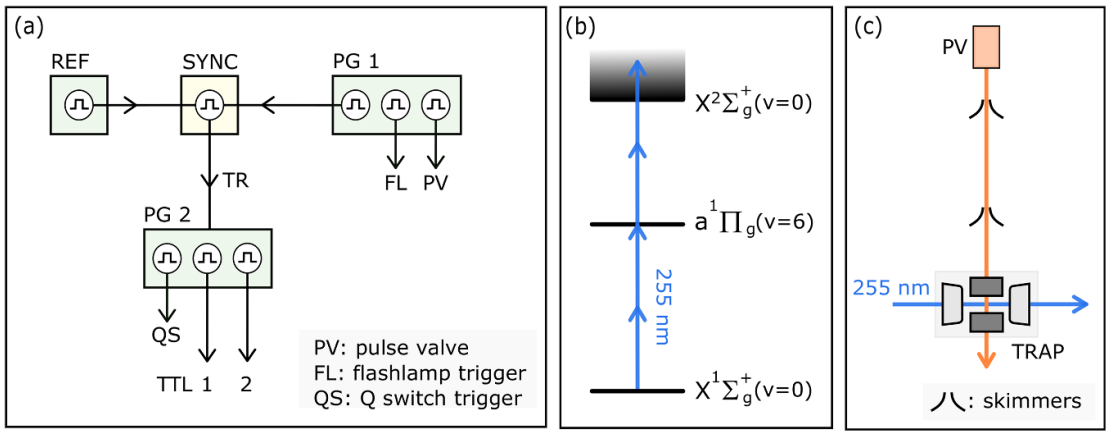

Figure 7. (a) Set-up used to capture nitrogen ions during switching of the rf trap drive. (b) Energy level diagram showing the 2+2 REMPI process to ionise nitrogen. (c) Set-up of the lasers and molecular beam.

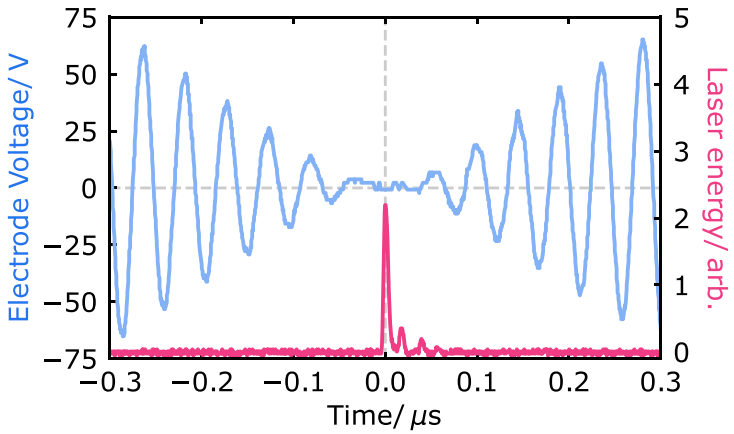

Figure 8. Example of ionisation laser pulse, synchronised to the minimum of the rf field during switching of the trap drive.

4. Capture of new ions

4.1. Methods

In the previous section, we demonstrated that the trapping field can be switched off without losing trapped ions. In this section, we have investigated whether ions can be loaded into the ion trap while the trapping field is minimised.

A crystal of calcium ions was prepared and weighed to determine the secular frequency of the pure $^{40}Ca^+$ crystal [33]. Nitrogen ions were then loaded into the ion trap via 2+2 REMPI from a skimmed molecular beam that passed radially through the trap (figure 7). The molecules were ionised [19] by a 6 ns laser pulse from a dye laser at 255 nm (Radiant Dyes Narrowscan), which was directed along the axis of the trap, perpendicular to the molecular beam. The composition of the ion crystal was monitored after the laser pulse using a CCD camera and, after the arrival of dark ions, the crystal was weighed again to determine the identity of any new ions that appeared in the crystal.

The trap was switched off such that the arrival of the laser pulse coincided with the minimum of the rf amplitude (e.g. figure 8). The radial secular frequency with normal operation was $2\pi\cdot(530 \pm 30)$ kHz and the trap was switched using the simple implementation with an extinction time of 1.080 μs and a recovery time of 1.475 μs.

4.2. Results and discussion

As a proof of principle, we were able to load N_2^+ ions into existing Coulomb crystals of $^{40}Ca^+$ ions via 2+2 REMPI using the switching technique (e.g. figure 9). In this process, the existing ions were retained and the newly formed ions were captured. This is in contrast to the normal procedure for loading ions, where the rf field is on throughout the process.

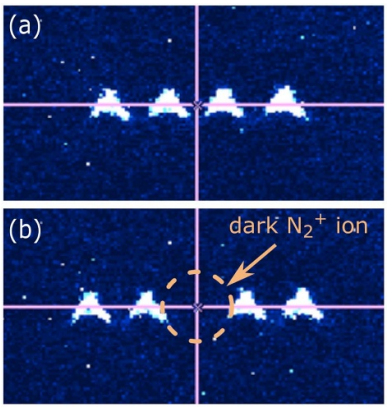

Figure 9. Example images showing the loading of a nitrogen ion into a Coulomb crystal of calcium ions. (a) A crystal of four calcium ions before the loading process. (b) The crystal after loading a single nitrogen ion into the crystal. In both cases, the pink cross marks the centre-of-mass of the crystal.

One potential use of this technique is to mitigate the field-induced broadening of the ionisation threshold which can inhibit state-selective ionisation of molecules in ion traps. We have shown that it is possible to load molecular ions into the trap by photoionisation while the trap field is extinguished. To prevent field ionisation, the trap must be switched off for longer than the lifetimes of the relevant Rydberg states, which are typically on the order of nanoseconds to microseconds for high-lying states [34]. We have shown in section 3 that it is possible to retain ions for several microseconds while the trap is off, which is likely to be long enough to satisfy this condition in many cases.

5. Conclusions

We have investigated the field extinction and ion dynamics during fast switching of the trapping field in an rf ion trap. By employing interference in the resonant circuit, we have shown that the trap can be switched off and on again within a few microseconds with an extinction ratio >50 dB, without the loss of ions. Additionally, we have shown that new ions can be loaded into the trap during the period when the rf field is extinguished. Whilst this method does cause heating of the ion crystal, careful choice of the switching and cooling parameters can minimise the recooling time.

This is a widely applicable technique that enables near-zero-field conditions in an rf ion trap. It therefore has the potential to improve processes that are adversely affected by the electric fields of the trap itself, such as state-selective loading of molecular ions. This is important in the building of molecular ion clocks for metrology and fundamental physics tests, and generating polyatomic molecular ions for applications including quantum-state-controlled chemical reaction studies, tests of parity violation and quantum computing.

Data availability statement

The data that support the findings of this study are openly available at the following URL/DOI: https://doi.org/10.25377/sussex.28054460.

Acknowledgments

This work was supported by the UK Science and Technology Facilities Council Grant ST/T006048/1.

Author contributions (CRediT)

Laura Blackburn: Conceptualisation, Investigation, Formal Analysis and Visualisation, Writing—Original Draft. **Amber Shepherd**: Writing—Review & Editing. **Matthias Keller**: Conceptualisation, Supervision, Writing—Review & Editing.

ORCID iDs

Laura Blackburn https://orcid.org/0000-0002-4746-7009
Amber Shepherd https://orcid.org/0000-0002-8901-0701
Matthias Keller https://orcid.org/0000-0002-3160-7396

References

[1] Häffner H, Roos C F and Blatt R 2008 Quantum computing with trapped ions *Phys. Rep.* **469** 155–203
[2] Bruzewicz C D, Chiaverini J, McConnell R and Sage J M 2019 Trapped-ion quantum computing: progress and challenges *Appl. Phys. Rev.* **6** 021314
[3] Ludlow A D, Boyd M M, Ye J, Peik E and Schmidt P O 2015 Optical atomic clocks *Rev. Mod. Phys.* **87** 637–701
[4] Brewer S M, Chen J-S, Hankin A M, Clements E R, Chou C W, Wineland D J, Hume D B and Leibrandt D R 2019 $^{27}Al^{+}$ quantum-logic clock with a systematic uncertainty below10^{-18} *Phys. Rev. Lett.* **123** 033201
[5] Schiller S, Bakalov D and Korobov V I 2014 Simplest molecules as candidates for precise optical clocks *Phys. Rev. Lett.* **113** 023004
[6] Safronova M S, Budker D, DeMille D, Jackson Kimball D F, Derevianko A and Clark C W 2018 Search for new physics with atoms and molecules *Rev. Mod. Phys.* **90** 025008
[7] Barontini G *et al* 2022 Measuring the stability of fundamental constants with a network of clocks *EPJ Quantum Technol.* **9** 12
[8] Heazlewood B R 2019 Cold ion chemistry within Coulomb crystals *Mol. Phys.* **117** 1–8
[9] Schmidt P O 2005 Spectroscopy using quantum logic *Science* **309** 749–52
[10] Chou C-wen, Kurz C, Hume D B, Plessow P N, Leibrandt D R and Leibfried D 2017 Preparation and coherent manipulation of pure quantum states of a single molecular ion *Nature* **545** 203–7
[11] Tsikritea A, Park K, Bertier P, Loreau J, Softley T P and Heazlewood B R 2021 Inverse kinetic isotope effects in the charge transfer reactions of ammonia with rare gas ions *Chem. Sci.* **12** 10005–13
[12] Kilaj A, Wang J, Straňák P, Schwilk M, Rivero U, Xu L, von Lilienfeld O A, Küpper J and Willitsch S 2021 Conformer-specific polar cycloaddition of dibromobutadiene with trapped propene ions *Nat. Commun.* **12** 6047
[13] Krohn O A, Catani K J, Sundar S P, Greenberg J, da Silva G and Lewandowski H J 2023 Reactions of acetonitrile with trapped, translationally cold acetylene cations *J. Phys. Chem.* A **127** 5120–8
[14] Patterson D 2018 Method for preparation and readout of polyatomic molecules in single quantum states *Phys. Rev.* A **97** 033403
[15] Landau A, Eduardus, Behar D, Ruth Wallach E, Pašteka L F, Faraji S, Borschevsky A and Shagam Y 2023 Chiral molecule candidates for trapped ion spectroscopy by ab initio calculations: from state preparation to parity violation *J. Chem. Phys.* **159** 114307
[16] King S A *et al* 2022 An optical atomic clock based on a highly charged ion *Nature* **611** 43–47
[17] Micke P, Leopold T, King S A, Benkler E, Spieß L J, Schmöger L, Schwarz M, Crespo López-Urrutia J R and Schmidt P O 2020 Coherent laser spectroscopy of highly charged ions using quantum logic *Nature* **578** 60–65
[18] Larson D J, Bergquist J C, Bollinger J J, Itano W M and Wineland D J 1986 Sympathetic cooling of trapped ions: a laser-cooled two-species nonneutral ion plasma *Phys. Rev. Lett.* **57** 70–73
[19] Gardner A, Softley T and Keller M 2019 Multi-photon ionisation spectroscopy for rotational state preparation of N_2^+ *Sci. Rep.* **9** 506
[20] Stollenwerk P R, Antonov I O and Odom B C 2019 IP determination and 1+1 REMPI spectrum of SiO at 210–220 nm in an ion trap: implications for SiO^+ ion trap loading *J. Mol. Spectrosc.* **355** 40–45
[21] Chupka W A 1993 Factors affecting lifetimes and resolution of Rydberg states observed in zero-electron-kinetic-energy spectroscopy *J. Chem. Phys.* **98** 4520–30
[22] Mackenzie S R, Merkt F, Halse E J and Softley T P 1995 Rotational state selectivity in N_2^+ X $^2\sigma_g^+$ ($v^+ = 0$) by delayed pulsed field ionization spectroscopy via the a′′ $^1\sigma_g^+$ ($v' = 0$) state *Mol. Phys.* **86** 1283–97
[23] Blackburn L and Keller M 2020 The effect of the electric trapping field on state-selective loading of molecules into rf ion traps *Sci. Rep.* **10** 18449
[24] Shlykov A, Roguski M and Willitsch S 2023 Optimized strategies for the quantum-state preparation of single trapped nitrogen molecular ions *Adv. Quantum Technol.* **8** 2300268
[25] Deb N, Pollum L L, Smith A D, Keller M, Rennick C J, Heazlewood B R and Softley T P 2015 Coulomb crystal mass spectrometry in a digital ion trap *Phys. Rev.* A **91** 033408
[26] Jones R M, Gerlich D and Anderson S L 1997 Simple radio-frequency power source for ion guides and ion traps *Rev. Sci. Instrum.* **68** 3357–62
[27] Chang B T and Mitchell T B 2006 Frequency stabilized radio-frequency generator for driving ion traps and other capacitive loads *Rev. Sci. Instrum.* **77** 063101
[28] Marmillod P, Antonioni S and Lorenz U J 2013 A radio frequency/high voltage pulse generator for the operation of a planar multipole ion trap/time-of-flight mass spectrometer *Rev. Sci. Instrum.* **84** 044707
[29] Neuwirth D, Eckhard J F, Lange K, Visser B, Wiedemann M, Schröter R, Tschurl M and Heiz U 2015 Using controlled ion extraction to combine a ring electrode trap with a reflectron time-of-flight mass spectrometer *Int. J. Mass Spectrom.* **387** 8–15
[30] Schneider C, Schowalter S J, Yu P and Hudson E R 2016 Electronics of an ion trap with integrated time-of-flight mass spectrometer *Int. J. Mass Spectrom.* **394** 1–8
[31] Wesenberg J H *et al* 2007 Fluorescence during Doppler cooling of a single trapped atom *Phys. Rev.* A **76** 053416
[32] Sikorsky T, Meir Z, Akerman N, Ben-shlomi R and Ozeri R 2017 Doppler cooling thermometry of a multilevel ion in the presence of micromotion *Phys. Rev.* A **96** 012519
[33] Sheridan K and Keller M 2011 Weighing of trapped ion crystals and its applications *New J. Phys.* **13** 123002
[34] Lefebvre-Brion H 1999 Lifetimes of Rydberg states in small molecules *The Role of Rydberg States in Spectroscopy and Photochemistry: Low and High Rydberg States* ed C Sandorfy (Kluwer)